BIOSYSTEMS ENGINEERING 110 (2011) 73–82

Available at www.sciencedirect.com

ScienceDirect

journal homepage: www.elsevier.com/locate/issn/15375110

Research Paper

Prediction of the contact area of agricultural traction tyres on firm soil

E. Diserens [a,*], P. Défossez [b], A. Duboisset [c], A. Alaoui [d]

[a] Agroscope Reckenholz-Tänikon ART Research Station, CH-8356 Ettenhausen, Switzerland
[b] INRA-Ephyse, 71 Avenue Edouard Bourlaux, BP 81, F-33883 Villenave d'Ornon Cedex, France
[c] Cemagref, TCF, Groupement de Clermont-Ferrand, 24 av. des Landais, BP 50085, F-63172 Aubière Cedex, France
[d] Hydrology Group, Department of Geography, University of Bern, Hallerstrasse 12, CH-3012 Bern, Switzerland

ARTICLE INFO

Article history:
Received 28 September 2010
Received in revised form
6 June 2011
Accepted 10 June 2011
Published online 3 August 2011

Equations were developed to enable reliable calculations to be made of the contact area for a wide range of traction tyres from independent easily accessible variables taken on firm ground. Given that when tyre size TS (section width [m] $\times$ outer diameter of tyre [m]), increases the specific contact area, A_s (ratio of the contact area to the tyre volume), decreases and tyre stiffness increases, it is worth taking into account tyre intrinsic properties by studying the impact of external constraints such as load and inflation pressure on the contact area. Based on a wide range of measurements (64, from a total of 28 tyres used on 12 grassland and open ground sites), three classes will be proposed for estimation of the contact area on firm agricultural soil: i) small tyres with $TS < 0.6$, ii) medium tyres with $0.6 \leq TS < 1.2$, and iii) large tyres with $TS \geq 1.2$. When considering not only TS but also load and inflation pressure as explainable variables, an increase in R^2 by 5% was observed. In addition, after taking into account intrinsic properties of the tyre, a new tyre classification has been proposed leading to an additional increase of R^2 by about 2%. Compatibilities with algorithms developed by other authors are discussed.

1. Introduction

The main dangers threatening agricultural land in recent decades are erosion, loss of organic material, and soil compaction especially in countries with mechanised agriculture (Jones, 2002). Field driving and field tilling with heavy machines contribute to soil compaction and soil shearing and reduce the storage and hence availability of oxygen, water, nutrients and heat to the soil (Tobias et al., 1999, p. 32), with a resulting crop yield decrease (Alakukku & Elonen, 1995; Coehlo, Mateos, & Villalobos, 2000; Davies, Finney, & Richardson, 1973; Gregory et al., 2007; Heinonen, Alakukku, & Erkki, 2002; O'Sullivan, Robertson, & Henshall, 1999). This affects the environment by increasing N_2O, CH_4 and CO_2 emanation from faded soils (Horn, Domzal, Slowinska-Jurkiewicz, & van Ouverkerk, 1995; Soane & van Ouwerkerk, 1994). It is therefore essential to estimate the tyre contact area concerned since this parameter appears in (i) the calculation of surface pressures (Döll & Schneider, 2001; Keller, 2005; Schjønning, Lamandé, Tøgersen, Arvidsson, & Keller, 2008), (ii) models of strain stress propagation in soil (Bastgen and Diserens, 2009; Smith, 1985; Söhne, 1953) and (iii) the prediction of severe risks of compaction (Défossez & Richard, 2002; Diserens, Chanet, & Marionneau, 2010; O'Sullivan, Henshall,

* Corresponding author. Tel.: +41 52 368 33 53; fax: +41 52 365 11 90.
E-mail address: etienne.diserens@art.admin.ch (E. Diserens).
1537-5110/$ – see front matter
doi:10.1016/j.biosystemseng.2011.06.008

Nomenclature

A	Contact area (measured or calculated), m^2
A_n	Contact area by testing the significance of each equation (dummy variable test)
A_s	Specific contact area, ratio between the measured A and the tyre volume V (tyre manufacturer values without tyre deflation), m^2 m^{-3}
a	Coefficient
b	Coefficient
c	Coefficient
D	Outer diameter of the unladen tyre, m
F	Static wheel load, kN
h_s	Width of spherical segment
K_c	Carcass stiffness of the tyre, kN m^{-1}
ΔK_p	Inflation pressure dependence, kN m^{-1} kPa^{-1}
K_t	Stiffness of the tyre, kN m^{-1}
P_i	Inflation pressure, kPa
PR	Penetration resistance, MPa
r	Radius of a theoretical sphere
R_d	Rim diameter, m
S_s	Outer surface of spherical segment
TS	Tyre size defined as the product of section width W and outer diameter D, m^2
V_s	Volume of spherical segment
V_t	Volume of the tyre without tyre deflation (tyre manufactuer values), m^3
W	Section width of the tyre, m
Y	Tyre age, years
α_n	Coefficient of regression after coupling the equations (dummy variable test)
β_n	Coefficient of regression by testing the significance of each equation (dummy variable test)

& Dickson, 1999; Van den Akker, 1998). Moreover, on farmland or on the road, contact area is also related to the forces acting on the wheel (traction force, rolling resistance, and braking force), determining vehicle grip, wear on tread, road safety, and fuel consumption (Döll, 1999; Eichhorn, 1999, p. 688; Rempfer, 1998). Contact area plays a major role in relation to the environment and to crop production.

There are numerous algorithms for estimating the contact area of traction tyres on agricultural ground, but only few equations give sufficiently reliable estimates for a wide range of tyres. They do not take into account the tyre volume and tyre stiffness that basically constitute reliable parameters allowing consistent classification. In general, the applicability of the equations suggested in the literature, is limited for several reasons: i) they need complementary in-situ measurements to precisely estimate the contact area, ii) are not precise enough because of the lack of the important variables, iii) give satisfactory results for only a narrow range of defined tyres, or iv) are applicable with uncommonly variables under undefined soil conditions. Previous studies have described contact area strictly on the basis of the measured contact dimensions and the unladen tyre radius (Schwieger, 1996), or the depth of the rut (Bolling, 1987). Although it is quite simple and is applied immediately after the passage of the machine, this model is unusable for the estimation of the contact area without additional in-situ measurements. The model fails to consider readily accessible parameters such as wheel load or inflation pressure. These two parameters together with the tyre size (TS) are decisive in characterising tyre deformation for a given speed on a defined ground (Lines & Murphy, 1991).

Simple formulae are used that take into account the diameter (D) and the width (W) of the tyre are available for tyres of high bearing capacity (Inns & Kilgour, 1978) and high and low bearing capacity (McKyes, 1985, p. 217). Although that these equations are widely used, they provide comparison between different tyres for a specific soil only with regard to the tyre dimension. According to Godin et al. (2006), the models considering only the size of the tyres for a defined soil (McKyes, 1985, p. 217) produce contact area values with large errors varying between 40 and 70%.

For a hard surface, Steiner (1979) selected four radial and nine diagonal tyres and developed two algorithms for cross-ply and radial tyres, with normal profiles (ratio between tyre height and section width $\geq$ 0.8), with inflation pressures ranging between 80 and 220 kPa and wheel loads between 5 und 25 kN, selecting as parameters the wheel load, tyre diameter and inflation pressure. The algorithms proposed by Steiner (1979) are precise but for a limited range of tyres, tyre loads and inflation pressures. In the Compsoil model, O'Sullivan, Robertson et al. (1999) used the same independent variables (overall width and diameter of tyre, static wheel load and inflation pressure) derived from unpublished data to calculate the contact area. In addition, they introduced a proportionality factor according to the soil hardness measured with bulk density at the soil surface considered as not easily accessible parameter. Komandi's approach (1990) is similar to the approach of O'Sullivan, Robertson et al. (1999). It contains a formula including a variable "soil coefficient" related to penetration resistance for medium firm soil, sandy stubble field and loosened sand. It should be mentioned that the formula is based on 8 cross-ply narrow tyres no longer on the market; consequently its application for tyres used today is limited. None of the above algorithms is based on a classification, making them less reliable for a wide range of traction tyres.

Comparing the shape of the contact area to an ellipse, Grecenko (1995) suggested multiplying the product of the length and the section width of the contact area by a coefficient varying between 0.8 and 0.9 (1 for a rectangle). The wheel load (load divided by maximum load at the given inflation pressure) was used as a correction factor. From measurements on rather soft ground, Keller (2005) considered the contact area as a super ellipse (as reported by Hallonborg, 1996) described by the width of the tyre and the length of the ellipse. The length is correlated with the diameter of the tyre and the pressure ratio (measured tyre pressure divided by recommended pressure for a given load and speed without explicitly considering the load). It is worth mentioning that with a predefined load and speed, the recommended pressure tends to decrease with new tyre generations (speed index D at

65 km h^{-1}) which makes this ratio rather uncertain. Both models require variables difficult to obtain. The above considerations led to the two following observations:

i) Load and inflation pressure are relevant and light accessible parameters for improving the contact area estimates.
ii) The use of equation without considering the intrinsic tyres properties is not sufficient to precisely estimate the contact area for the wide range of current agricultural traction tyres for given soil conditions.

The aim of this study is to propose reliable algorithms to better predict the contact area for a wide range of current agricultural traction tyres in the same way as for trailer tyres (Diserens, 2009) under defined firm soil conditions, taking into account easily accessible explanatory variables such as *TS*, load, and inflation pressure. The limits between the tyre groups were set in respect to their sizes or intrinsic properties to neutralise the inherent influences on the contact area and consequently to reinforce the important variables such as load and inflation pressure.

2. Theoretical basis

A reliable classification as based on the tyres properties may provide a better estimation of the influence of the wheel load and the inflation pressure on the contact area. These intrinsic properties can be defined by geometrical and constitutive characteristics of the tyres.

2.1. Geometrical properties

By analogy, a given tyre is considered to be a spherical segment with a section width h_s and radius r (Fig. 1).

The basic formulae to calculate the surface of a spherical segment S_s is:

$$S_s = 2\pi r h_s \quad (1)$$

The equation defining the volume of a spherical segment, where r_1, r_2 are the radii of the two bases with same sizes, is:

$$V_s = \frac{\pi}{6}\left(3r_1^2 + 3r_2^2 + h_s^2\right)h_s \quad (2)$$

For a defined relationship between section width h_s and a radius r ($h_s = 1/2\ r$), the ratio of the spherical surface segment S_s to the spherical volume segment V_s decreases exponentially when the radius of the sphere r increases (Fig. 2). By analogy to this, the relation between the *TS* (i.e. section width W × outer diameter *D*) and the contact area is also not linear.

2.2. Constitutive characteristics

The tyre stiffness (K_t) is the rate of change of the restoring force with deflection. The factors which have a large effect on the stiffness are the inflation pressure, the section width of the tyre, the rim diameter and tyre age (Eq. (3c)). According to Lines and Murphy (1991), the stiffness of a rolling tyre is usually lower than that of a stationary tyre. Stiffness decreases significantly with increasing speed for low speed range (<10 km h^{-1}). For higher speed ranges, stiffness does not vary significantly. Neglecting the impact of the speed, Lines and Murphy (1991) provided an equation (Eq. (3)) to calculate K_t:

$$K_t = K_c + P_i \Delta K_p \quad (3)$$

with the carcass stiffness of the tyre (K_c), kN m^{-1} given by:

$$K_c = 1.72 - (69.69\ R_d) + (5.6Y) \quad (3a)$$

and the inflation pressure dependence (ΔK_p), kN m^{-1} kPa^{-1} given by:

$$\Delta K_p = 5.27W\ R_d \quad (3b)$$

The tyre stiffness kN m^{-1} is calculated as:

$$K_t = 1.72 - (69.69\ R_d) + (5.6Y) + (5.27W\ R_d P_i) \quad (3c)$$

where R_d is rim diameter (m), Y is tyre age (years), W is section width of the tyre (m), and P_i is inflation pressure (kPa).

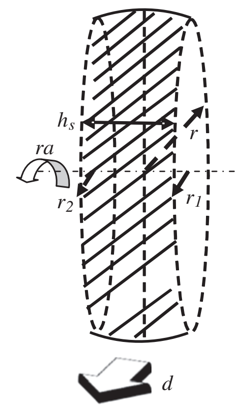

Fig. 1 – Wheel represented by a spherical segment. h_s is the width and r_1 and r_2 are the bases inserted in a sphere with radius r and rotation axle *ra*. Hatched section represents the outer surface of the spherical; *d* represents driving direction.

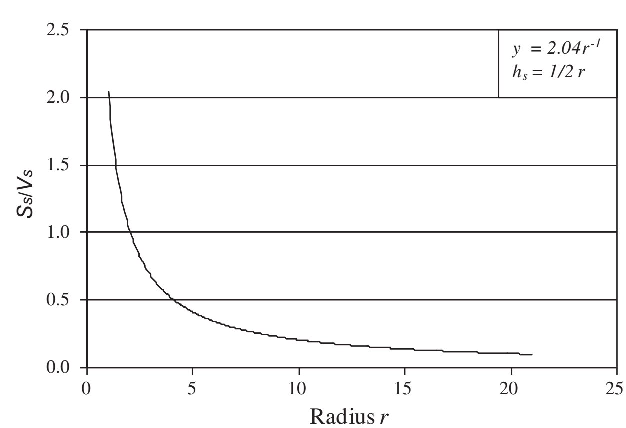

Fig. 2 – Relationship between radius r and ratio of spherical segment surface S_s to its volume V_s for the height of the spherical segment h_s = ½ r.

The relationship between tyre stiffness and *TS* for four defined P_i levels is given in Fig. 3. A mean age of five years was assumed for the tyres considered. Lines and Murphy (1991) observed that the carcass stiffness K_c decreases when the rim diameter increases (Eq.(3a)). Conversely, both ΔK_p (Eq. (3b)) and K_t (Eq. (3c)) drastically increase when *TS* increases (for a defined P_i), or when the P_i increases (for a defined *TS*) (Fig. 3).

Since the ratio of a spherical segment surface to its spherical segment volume and the tyre stiffness change with the tyre dimensions, there is a need to classify the tyres according to their dimensions in order to neutralise the effect of the intrinsic properties before assessing the influence of external parameters such as load and P_i on the contact area.

3. Materials and methods

3.1. Experimental conditions and technical data

The measurements of the contact area were carried out on 12 plots with different textures, including loamy sand, loam, silt loam and clay loam. Three plots of ploughed or tilled soils, covered with sown meadow and maize straw, and four plots of natural meadow among which one was used four times under variable penetration resistance conditions, were considered in this study.

The machines used included two combine harvesters (132–221 kW), one beet harvester (235 kW) and 16 tractors (36–220 kW). The database includes a total of 28 tyres: nine tyres including one steering tyre and eight traction tyres with small diameters (<1.3 m, series 16, 24, 26.5, 28 - diameter of wheel rim in inches), four tyres with normal profiles (series 34, 36), and 15 low-profile tyres (series 24, 26, 28, 30, 32, 34, 38) (Table 1). The measurements of the contact area considered in this study were performed on plots without traffic. The rear wheels (series 32–38) rolled on the same tracks as the front wheels (series up to 30). Most of the tyres were subjected to different loads with different related P_i, recommended by the tyre manufacturers for speeds of 10 and 30 km h^{-1}. In practice, the greater the tyre dimensions, the lower the recommended P_i for a given wheel rim size and load. In this study, a total of 64

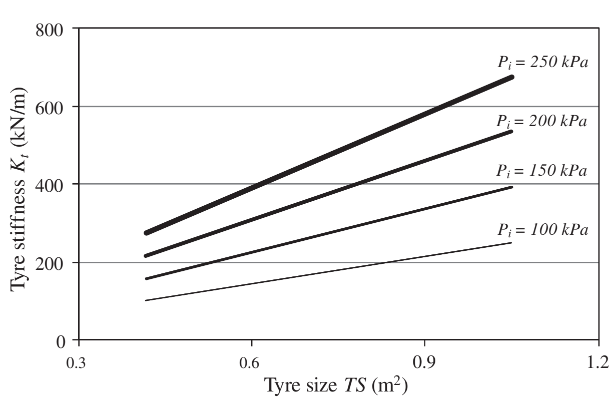

Fig. 3 – Relationship between tyre stiffness K_t and tyre size *TS* (*TS* is tyre section width *W* (m) × outer diameter *D* (m)) for different inflation pressures according to the Eq. (3c) from Lines and Murphy (1991) using the presented dataset.

measurements were made of which 60 were with radial traction tyres, currently the most representative tyre in crop and grassland farming.

3.2. Measurements

Given that the consistency of soil varies with soil texture, water content and plant cover, the penetration resistance *PR* or surface hardness of the soil is an appropriate parameter to describe the bearing capacity or consistency of the soil (Bueno, Amiama, Hernanz, & Pereira, 2006). This parameter was measured using a penetrometer provided with a compression spiral spring (max. 19.6×10^{-2} kN, type 800/20/4, manufactured by Pesola in Baar, Switzerland) and a screwdriver head (width 6 mm, head thickness 1 mm, and shaft diameter 4 mm) (Bastgen & Diserens, 2009). Two additional penetrometers were also considered for determining comparable ranges of resistance. A spring penetrometer with a 30° cone and 1 cm^2 base area (Walczak, Orlowski, & Pukos, 1973) and the penetrologger set PANDA (probe for automatic, numeric, dynamic computer-assisted penetrometry) (Gourves, 1996). At least 25 measurements distributed over five sectors were carried out on each plot. The values of the *PR* (cited below) were recorded during each penetration of the shaft between 0 and 0.1 m, which belongs to the plough layer localized between 0 and 0.2 m depth (Diserens & Steinmann, 2002). The penetration resistance was measured on firm soil (high bearing capacity) with a screwdriver penetrometer. Table 2 shows a comparison between the screwdriver penetrometer used in this study and the conventional ones. Because of the low head contact of a screwdriver, the calculated pressure is higher than by using other penetrometer types. Corresponding units for different penetrometers are given in Table 2 too.

The tyre loads were measured with mobile, flat-bed wheel-load scales (type Haenni WL 103, Jegenstorf, Switzerland) that can record loads of up to 10^2 kN (accuracy $\pm 13 \times 10^{-2}$ kN). The tyre P_i were measured with a pressure meter (type MotoMeter, Germany, maximum value 4.5×10^2 kPa, accuracy $\pm$ 2 kPa).

Measurements of contact area were carried out using a photometric method (using a two-dimensional projection of the actual static surface area when the tyre is stationary). On the meadow, the plant cover was first cut using a mower, followed if necessary by a second cut with a mower. The print circumference of the tyre on the ground was first sprinkled with calcium oxide powder. Then bellows were used to distribute the powder around and beneath the tyre between the lugs (interstices, undertread spaces) so as to fill the maximum free space around and below the tyre. This is particularly significant for hard ground as described by Diserens (2009). Two rules were placed on the edge of the print area in the *x*- and *y*-direction once the load has been removed to serve as reference and to control also the distortion of the slides, which appears to be negligible. The contours were photographed with a digital camera (Canon Power Shot G5, resolution: 5 Mega pixels, 118 pixels/10^{-2} m). By means of a ladder, it was possible to adjust the camera to a sufficient height (between 0.9 m and max. 1.3 m) for the largest print area. The position of the contour on the slide was then optimised by positive or negative zooming. Print area was then analysed by photometry using Adobe Photoshop Elements software (Version 2.0) (Diserens, 2002, p. 12).

Table 1 – Tyre data on firm soil.[a]

Tyre description	Tyre volume (m^3)	Tyre width (m)	Outer diameter (m)	Wheel load range (kN)	Inflation pressure range (kPa)	Number of measurements (n) $\Sigma = 64$
7.50–16	–	0.19	0.81	3.68	100	1
14.9/13-24	–	0.38	1.27	10.40	130	1
8.3 R 24	0.0653	0.21	0.99	4.61–4.22	60–200	2
13.6 R 24	0.1813	0.35	1.19	9.22	120	1
380/85 R 24	0.2280	0.38	1.26	8.63–8.73	60–200	2
380/85 R 24	0.2280	0.38	1.26	7.75–7.95	60–200	2
420/70 R 24	0.2400	0.42	1.24	8.34–11.18	60–160	4
480/65 R 24	0.2600	0.48	1.23	8.34	80–150	2
540/65 R 24	0.3493	0.54	1.31	15.11	80–200	2
540/65 R 24	0.3493	0.54	1.31	10.10	90	1
540/65 R 26	0.4053	0.54	1.36	10.20	80–150	2
500/60–26.5	0.3467	0.50	1.26	28.84–30.02	100–240	2
11.2 R 28	0.1240	0.28	1.22	3.43	120	1
540/65 R 28	0.3920	0.54	1.41	14.42–13.93	60–140	2
600/65 R 28	0.5013	0.60	1.49	16.68–18.15	115–180	2
620/75 R 30	0.6747	0.62	1.69	17.56	100	1
800/65 R 32	0.9893	0.80	1.86	54.64–58.66	100–160	2
16.9 R 34	0.3867	0.43	1.58	14.52–14.13	120–220	2
16.9 R 34	0.3867	0.43	1.58	10.40–16.28	120–220	4
460/85 R 34	0.4547	0.46	1.66	16.87–15.30	60–160	2
520/70 R 34	0.5040	0.52	1.64	24.23–23.84	70–160	2
540/65 R 34	0.4480	0.54	1.57	25.75	80–160	2
600/65 R 34	0.6067	0.60	1.64	14	80–150	2
710/75 R 34	1.1507	0.71	1.95	57.19–92.70	180–320	2
9.5 R 36	0.1507	0.24	1.35	11.58–12.16	80–200	2
9.5 R 36	0.1507	0.24	1.35	10.10–10.50	120–210	2
13.6 R 36	0.2693	0.35	1.51	15.99	100–150	2
15.5 R 38	0.3013	0.39	1.57	15.79	80–160	2
600/65 R 38	0.6613	0.60	1.75	22.71–23.05	80–150	2
600/65 R 38	0.6613	0.60	1.75	20.80	110	1
650/65 R 38	0.8120	0.65	1.84	21.88–22.07	60–150	2
710/70 R 38	1.0200	0.71	1.93	106.78	190–300	2
710/70 R 38	1.0200	0.71	1.93	46.60–48.56	110–170	2
800/70 R 38	1.3267	0.80	2.07	38.85	160	1

a Plant cover, soil types, corresponding penetration resistance values of the used machines are available under request.

This print area was defined as the measured contact area *A*. One measure of the contact area was carried out for each tyre, load and pressure. To check the variability of the contour area on the field, three replications were made with one tyre (16.9R34) under two different load conditions (10.6 kN/120 kPa–10.4 kN/220 kPa).

3.3. *Measurements of intrinsic properties of traction tyre*

Analogous to a spherical segment (Fig. 2), surface and volume were also considered by means of a new parameter: the specific contact area A_s depending from the TS (Fig. 5). This parameter is expressed as follows:

Table 2 – Comparison between the screwdriver penetrometer (static) used in this study and the conventional ones (static and dynamic).

	Area of head (m^2)	Shaft diameter (m)	Hardness of the soil		
			soft	medium	hard
Static penetrometer, screwdriver (kN)[a]	6×10^{-6}	4×10^{-3}	0–0.05	> 0.05–0.08	>0.08
Static penetrometer, screwdriver (MPa)[b]	6×10^{-6}	4×10^{-3}	0–8.2	> 8.2–13.1	>13.1
Static penetrometer, screwdriver (MPa)[c]	6×10^{-6}	4×10^{-3}	0–4.0	> 4.0–6.4	>6.4
Static penetrometer, type Walczak (MPa)	100×10^{-6}	–	0–1.35	> 1.35–2.20	>2.20
Dynamic penetrometer, type Panda probe (MPa)	200×10^{-6}	–	0–1.0	> 1.0–1.6	>1.6

a measured values in kN.
b calculated values in MPa according to the head surface.
c calculated values in MPa according to the shaft section surface.

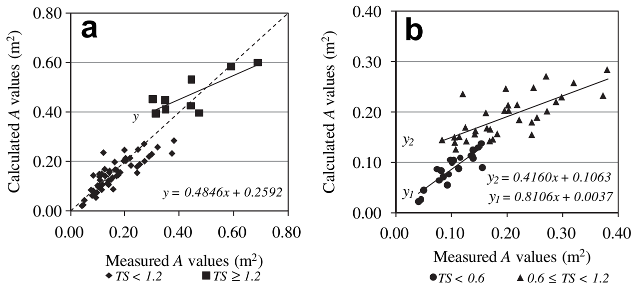

Fig. 4 – Calculated contact area values with the undifferentiated Eq. (14) (Table 3) compared a) to measured contact area values considering all data (presented in Table 1); – Line 1:1 and trend line y - and b) to measured contact area with tyre size *TS* (*TS* is section width *W* (m) × outer diameter *D* (m)) < 1.2; – Trend lines y_1 and y_2.

$$A_s = \frac{A}{V_t} \tag{4}$$

where A is the measured contact area by recommended load and P_i at 30 km h^{-1} and V_t is the volume of the tyre.

Twenty values of the contact area with low load and high P_i (recommended load and P_i for 30 km h^{-1}) measured on firm soil were selected to serve as references to avoid exaggeration in the distortion values, which would make comparison A_s unrepresentative (high deflation by high loads and low pressure). The corresponding values of V_t were given in the technical guidelines issued by the tyre manufacturers. The K_t of the sample data ($n = 64$) was calculated using the equation of Lines and Murphy (1991), where a mean age of five years was selected (Eq. (3c)). The relationship between the two intrinsic parameters (A_s, K_t) and TS was used as basis for a new classification to estimate the contact area.

3.4. *Statistics*

The significance of the classification according to TS on the basis for A_s and K_t values was tested by means of the non-parametric Kruskal–Wallis test (median significance test for more than two independent samples) since the values were not normally distributed.

For estimating the A for traction tyres on firm soil, relationships were then obtained by simple (Eq. (5)) or multiple linear regressions (Eq. (6)) with linear transformation (Diserens, 2009) in the form:

$$A = aX_1 \tag{5}$$

or in the form:

$$A = aX_1 + bX_2 + cX_3 + C \tag{6}$$

Where a, b, and c are constants, with independent explanatory factors: X_1: TS; X_2: wheel load; X_3: P_i with a constant C set to 0 because both measured and calculated data are close to the 1:1 line and zero.

The standard equation (Eq. (5)) has the advantage of comparing only the contact area for two tyres, taking into account only the size (excluding load and P_i). The degree of independence of each variable X_1, X_2 and X_3 was tested using a correlation matrix.

To test the significance of each equation two by two, a single regression (Eq. (9)) was run, using all the observations from each pair of compared equations Eqs. (7) and (8), measuring the effect of the qualitative factor (dummy variable), which is different for each equation ($\delta = 0$ or 1). The p-value of this qualitative factor δ is then determinant.

$$A_1 = \beta_1 X_1 + \beta_2 X_2 + \beta_3 X_3 \tag{7}$$

$$A_2 = \beta_1' X_1 + \beta_2' X_2 + \beta_3' X_3 \tag{8}$$

$$A_{12} = \alpha_1 X_1 + \alpha_2 X_2 + \alpha_3 X_3 + \delta \tag{9}$$

The Statistica software package (Stat Soft, Inc. STATISTCA Application Version 9.1.2010 Edition, Tulsa, OK, USA) was used for the statistical processing. Statistical analysis covered a total of 64 measurements.

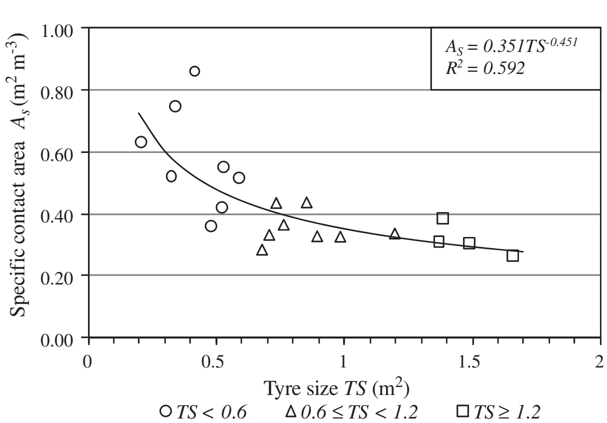

Fig. 5 – Relationship between tyre size *TS* (*TS* is section width *W* (m) × outer diameter *D* (m)) and specific contact area A_s.

4. Results and discussion

4.1. *Classification and relationships*

Firstly, the variability of the contour area was checked on the field with the 16.9 R 34 tyre with three replications under two different load conditions. In both cases, the variation coefficient was less than 5% (4.5% and 2.8% respectively) and was considered negligible compared with variation associated with multiple regression calculations varying between 10 and 20%.

The values covering all measurements were collected for the regression analysis with three variables, TS, wheel load and P_i (Eq. (14), Table 3). Comparison between measured and calculated values is given in Fig. 4a) with the line 1:1 ($R^2 = 0.951$). Two strong different clouds of points divide the graph. For low tyre dimensions, the points are in the direct vicinity of the line but under it. For tyres with high dimensions, the variations along the x axis are much higher than the variations along the y axis (Fig. 4a). In fact, the trend line y had lower slope than the line 1:1. Similarly, the trend line y_2

Table 3 – Multiple regressions. Formulae for calculating the contact area in firm soil for agricultural traction tyres with corresponding statistics - A (m^2): contact area, TS (m^2): tyre size or product of section width of tyre W (m) × outer diameter of tyre D (m), F (kN): tyre load, P_i (kPa): inflation pressure, R^2 (%): coefficient of determination, F-value: index of significance of the coefficient of determination, p-value (%): probability that the null hypothesis is true.

Tyre classes	Equations	Eq.	Statistics					
			n	R^2	F-value	p-values		
						TS	F	P_i
Equations of form $A = a\ TS$								
Undifferentiated	$A = 0.2692\ TS$	(10)	64	0.898	565.5	0.000		
$TS < 0.6$	$A = 0.2461\ TS$	(11)	22	0.958	505.5	0.000		
$TS \geq 0.6$ or < 1.2	$A = 0.2461\ TS$	(12)	33	0.902	303.7	0.000		
$TS \geq 1.2$	$A = 0.3031\ TS$	(13)	9	0.894	77.2	0.000		
Equations of form $A = a\ TS + b\ F + c\ P_i$								
Undifferentiated	$A = 0.180\ TS + 3.6 \times 10^{-3}\ F - 15.5 \times 10^{-5}\ P_i$	(14)	64	0.951	414.2	0.000	0.000	0.092
$TS < 0.6$	$A = 0.191\ TS + 4.6 \times 10^{-3}\ F - 14.8 \times 10^{-5}\ P_i$	(15)	22	0.973	260.0	0.000	0.004	0.031
$TS \geq 0.6$ or < 1.2	$A = 0.130\ TS + 9.2 \times 10^{-3}\ F - 53.5 \times 10^{-5}\ P_i$	(16)	33	0.961	270.1	0.000	0.000	0.000
$TS \geq 1.2$	$A = 0.126\ TS + 5.9 \times 10^{-3}\ F - 75.7 \times 10^{-5}\ P_i$	(17)	9	0.968	92.7	0.053	0.010	0.234

($0.6 < TS < 1.2$) has a lower slope than the y_1 ($TS < 0.6$) (Fig. 4b). These observations show that Eq. (14) (Table 3) does not describe the contact area for high TS values with enough precision. From Fig. 4a) and 4b) it appears that the contribution of the wheel load and the P_i for estimating the contact area increases when the TS increases. When gathering all the tyres for the regression analysis, it appears that the impact of size dissimulates the impact of the other explainable variables. To improve the estimate of the contact area which can also be revealed by the increase of R^2, regression analysis could be repeated for different classes of traction tyre. By taking into account the intrinsic properties of the tyre, new classes can be defined.

Analogy in the relationships between the spherical radius r and ratio of spherical segment surface S_s to its volume V_s and between A_s and TS appears (Figs. 2 and 5). On the one hand, ratio of spherical segment surface to its volume drastically decreases with increasing radius, on the other hand, specific contact area decreases similarly with TS. A first group ($TS < 0.6$) for which the size plays a major role in the specific area A_s estimates can be identified. Considering the relationship between TS and the tyre stiffness presented in Fig. 6, it appears that tyre stiffness increases when TS increases, which is foreseeable with commonly higher loads. The stiffness variation from 200 to 1200 kN m^{-1} (1:6) remains at a lower ratio compared to the maximum wheel load variations varying between 4 and 105 kN (1:26) at a speed of 10 km h^{-1} (Table 1).

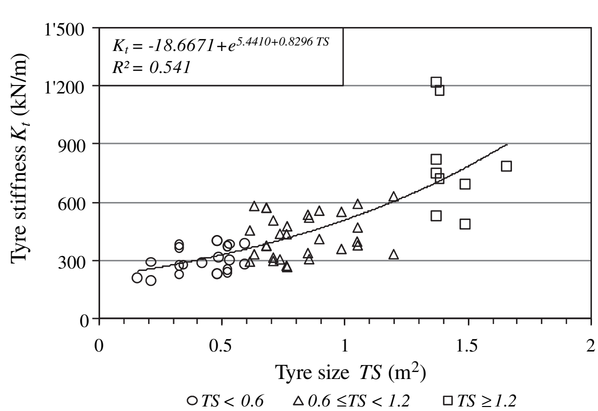

Fig. 6 – Relationship between tyre size TS (TS is section width W (m) × outer diameter D(m)) and the tyre stiffness K_t.

Because the great load increase is generally accompanied by an increase of TS, tyre deformation increased despite greater stiffness. This was particularly true for tyres with size $TS > 1.2$. Moreover, the influence of the P_i on the stiffness increases with the TS (Fig. 3). The tyre reaction on the contact area after considering the TS (Fig. 5), wheel load (Fig. 6) and P_i (Fig. 3) was not homogeneous and requires finer classification.

Taking into account the considerations above, three groups were qualitatively distinguished and were further statistically confirmed by means of regression analysis. The three groups were proposed as follows:

i) small tyres with $TS < 0.6$ corresponding to a maximum wheel load of about 30 kN;
ii) medium tyres $0.6 \leq TS < 1.2$ corresponding to a maximum wheel load of about 65 kN; and
iii) large tyres with $TS \geq 1.2$ corresponding to a maximum wheel load of about 115 kN; all load values at 10 km h^{-1}.

In Table 4, the significance of both A_s and K_t for each group is given. The three groups are significantly different. Only in one case there was no significance found between the contact areas of medium and large tyres probably resulting from the drastic decrease of A_s appearing only for low $TS < 0.6$ (Fig. 5).

According to this classification, a separate regression analysis was conducted for each group (Eqs. 15, 16 and 17, Table 3). Thus, the estimation of contact area was improved as shown by the high value of R^2 exceeding 0.95. From this analysis, it appears clearly that the impact of the TS on the contact area for low TS (<0.6) is important (p-value = 0), while the impact of the load and the P_i on the contact area is weaker but also significant (p-values < 0.05). The coefficient of regression (a) related to the TS for this group comparing to the others groups is also the highest (Eq. (15), Table 3).

The significance of these three equations was checked with the dummy variable test (Table 5). In two by two comparisons,

Table 4 – Specific surface and tyre stiffness. Medians from the three classes of tyres and *p* - values (Kruskal–Wallis Test), *TS*: Tyre size represented by the product width (m) and outer diameter (m).

	$TS < 0.6$ $n = 8/22$	$TS \geq 0.6$ and <1.2 $n = 8/33$	$TS \geq 1.2$ $n = 4/9$
Specific surface (A_s), medians ($m^2\ m^{-3}$)	0.537	0.332	0.307
$TS < 0.6$ (*p*-values)	–	0.030	0.007
$TS \geq 0.6$ and <1.2(*p*-values)	–	–	1.000
Tyre stiffness (K_t), medians ($kN\ m^{-1}$)	241.87	331.19	691.71
$TS < 0.6$ (*p*-values)	–	0.001	0.000
$TS \geq 0.6$ and <1.2(*p*-values)	–	–	0.005

Table 5 – Test of significance between equation 15–17 (Table 3), *p* -values from dummy variable *δ*, *TS*: Tyre size represented by the product width (m) and outer diameter (m).

Tyre profile	$TS < 0.6$ $n = 22$	$TS \geq 0.6$ and <1.2 $n = 33$	$TS \geq 1.2$ $n = 9$
$TS < 0.6$	–	0.073	0.027
$TS \geq 0.6$ and <1.2	–	–	0.000

all the *p*-values are less than 0.1. The intrinsic properties of the tyres, such as specific area or stiffness, play a major role on contact area. Examination of the test of correlation shows that the three explainable variables were highly independent (Table 6). Only in one case, for the largest tyres, did the test of correlation give a positive correlation (0.75) between load and P_i, probably due to the low data sample with different loading under constant P_i and/or the large variation in the load and in the P_i, also leading to a high *p*-value (0.23) for P_i (Eq. (17), Table 3). By including additional data from large tyres (section width × diameter ≥ 1.2), the estimation of contact area can probably be improved. Except for the P_i of the largest tyre group, all the coefficients of regression related to the explainable variables (*TS*, load and P_i) were significant (*p*-values < 0.10).

The statistical analysis of the simple and multiple linear regressions (Eqs. 10–17) given in Table 3 clearly confirms: (i) the importance of the load and the P_i on the estimation of the contact area, especially for $TS \geq 0.6$ shown by the increase of R^2 up to 5% and (ii) the importance of a preliminary classification of the traction tyre according to size shown by an additional increase of R^2 up to 2%.

Table 6 – Correlation matrix between the explainable variables, *TS*: Tyre size represented by the product width (m) and outer diameter (m).

	$TS < 0.6$ $n = 22$	$TS \geq 0.6$ and <1.2 $n = 33$	$TS \geq 1.2$ $n = 9$
Tyre sizes vs. load	0.50	0.30	−0.52
Tyre sizes vs. inflation pressure	−0.09	−0.27	−0.33
Load vs. inflation pressure	0.08	0.01	0.75

4.2. *Comparisons with other studies*

Comparisons were carried out between the proposed empirical equations based on tyre classification and equations or measurements from other studies that do not distinguish explicitly between tyre groups. Several published formulae for calculating the contact area for farming traction tyres on soft and firm soils are compiled in the Appendix.

Introducing measured values from Godin (2005) for small tyres ($TS < 0.6$) into Eq. (15) (Table 3), the group of the obtained values did not diverge significantly from the data proposed in this study (Fig. 7).

Comparing the contact area measurements with the values calculated using Steiner's equation (Eq. (25), Appendix), a satisfactory juxtaposition of the points was observed in the low range (Fig. 8). The two sets of data with corresponding trend lines y_1 and y_2 are similar, although the accuracy of the new model is higher (Fig. 8). The relative mean difference between the two calculated values was 19.1%. Steiner's formula used here for standard radial tyres with normal profile (ratio height/section width = 0.82) suits a hard soil (high bearing capacity). At low P_i (60 kPa), with a contact area of 0.38 m^2 (single measure in Fig. 8), Steiner's equation overestimates measured contact area by 84%. The deviation decreases to 14.8% when Eq. (16) is used (Table 3). Measurements with low P_i (<80 kPa) led to overestimated values. In summary, it may be concluded that for large tyres, the

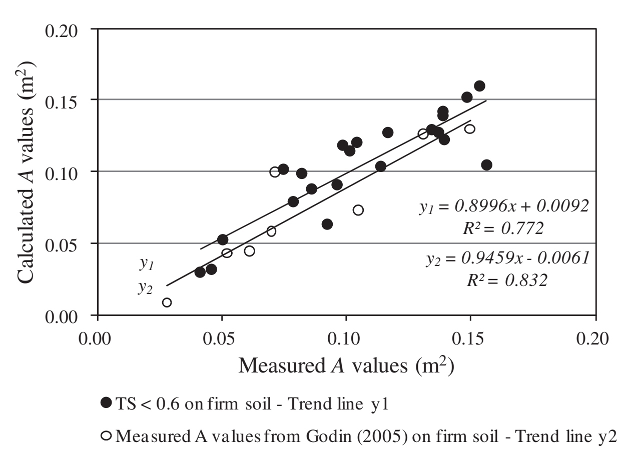

Fig. 7 – Validation of Eq. (15) (Table 3) for tyre size *TS* < 0.6 (*TS* is section width *W* (m) × outer diameter *D* (m)) with measured contact area values obtained from Godin (2005) on firm soil; – Trend lines.

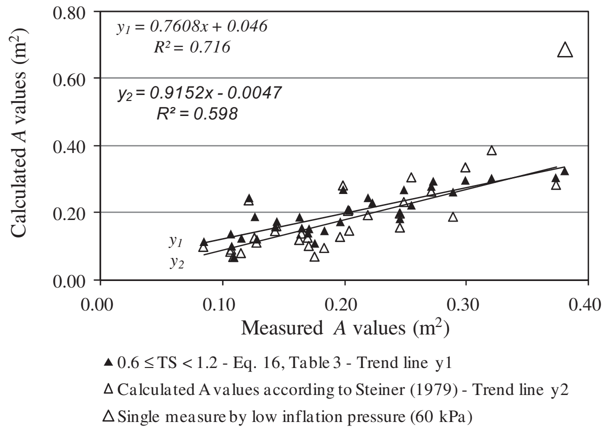

Fig. 8 – Comparison between calculated contact area values according to Eq. (16) (Table 3) and the values according to Steiner (Appendix, Eq. (25)) for radial tyres with tyre size 0.6 ≤ *TS* < 1.2 on firm soil. (*TS* is section width *W* (m) × outer diameter *D* (m)); – Trend lines.

Steiner's model is not suitable for new traction tyres with high load ability (load index) under low P_i.

On a very hard ground (bulk density of 1.8), the obtained values using O'Sullivan's model (Eq. (27), Appendix) were lower than those calculated with Eqs. (16) and (17) (Table 3), especially for large tyres (Fig. 9). The relative mean difference between the two calculated values exceeds 30% (33.6%) with a maximum value up to 52.3%. These results highlighted the large discrepancies between the two models. O'Sullivan, Robertson et al. (1999) suggest linear extrapolation of regression coefficients, an impossible method to circumvent, which requires soil bulk density analyses in a majority of the cases.

Rigorous parameterisation of soil penetration resistance as an easily accessible explanatory variable requires further research with an appropriate experimental procedure.

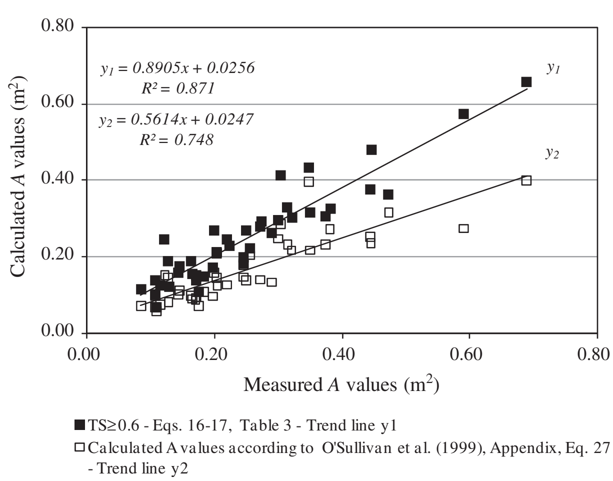

Fig. 9 – Comparison between calculated contact area values according to the Eqs. 16 and 17 (Table 3), *TS* ≥ 0.6 (*TS* is section width *W* (m) × outer diameter *D* (m)) and the values calculated according to O'Sullivan (Eq. (27), Appendix) for firm soil; – Trend lines.

5. Conclusions

The regression analysis shows that the best estimation of the contact area was obtained by considering not only explainable variables as *TS* (width (m) × diameter (m)), load and inflation pressure P_i but also the intrinsic properties of the tyre. Intrinsic properties such as specific contact area A_s and tyre stiffness K_t are not homogeneous within the wide range of tyres and consequently indirectly influence the analysis. Therefore, three distinct tyre groups were suggested for the regression analyses: (i) traction tyres with $TS < 0.6$, (ii) traction tyres with $TS \geq 0.6$ and <1.2, and (iii) traction tyres with $TS \geq 1.2$. Additional data samples for the last groups ($TS \geq 1.2$) were convenient to improve the low significance level of the P_i as explainable variable in the regression analysis.

Algorithms from other authors have been compared with the proposed ones and discussed with regard to their restrictive areas of application.

A detailed parameterisation of the soil penetration resistance is required to show its quantitative impact on the contact area. Because rapid development of new tyres is continually in progress, particularly with respect to their load capacity, regular updating of the algorithms is recommended.

Acknowledgements

We gratefully acknowledge the contributions of all the agricultural contractors who were willing to lend their machines for the contact area measurements. We thank also PhD Francesca Opsi (Institute for Agricultural and Earth Moving Machines National Research Council, Torino) for the comparative measurements of the penetration resistance (i.e. screwdriver and Walczak penetrometers).

Appendix. Supplementary material

Supplementary data associated with this article can be found, in the online version, at doi:10.1016/j.biosystemseng.2011.06.008.

REFERENCES

Alakukku, L., & Elonen, P. (1995). Long-term effects of a single compaction by heavy field traffic on yield and nitrogen uptake of annual crops. *Soil Tillage Research, 36*, 141–152.

Bastgen, H. M., & Diserens, E. (2009). q value for calculation of pressure propagation in arable soils taking topsoil stability into account. *Soil Tillage Research, 102*, 138–143.

Bolling, I. (1987). Bodenverdichtung und Triebkraftverhalten bei Reifen – Neue Mess- und Rechenmethoden – Forschungsbericht Agrartechnik des Arbeitskreises Forschung und Lehre der max-Eyth-Gesellschaft (MEG) 133. Dissertation, Munich.

Bueno, J., Amiama, C., Hernanz, J. L., & Pereira, J. M. (2006). Penetration resistance, soil water content, and workability of grasslands soils under two tillage systems. *Transactions of the ASABE, 49*(4), 875–882.

Coehlo, M. B., Mateos, L., & Villalobos, F. J. (2000). Influence of a compacted loam subsoil layer on growth and yield of irrigated cotton in Southern Spain. *Soil Tillage Research, 57*, 129–142.

Davies, D. B., Finney, J. B., & Richardson, S. J. (1973). Relative effects of tractor weight and wheelslip in causing soil compaction. *Journal of Soil Science, 24*(3), 399–409.

Défossez, P., & Richard, G. (2002). Models of soil compaction due to traffic and their evaluation. *Soil Tillage Research, 67*, 41–64.

Diserens, E. (2002). *Ermittlung der Reifen-Kontaktfläche im Feld mittels Rechenmodell*. FAT-Berichte Nr. 582.

Diserens, E. (2009). Calculating the contact area of trailer tyres in the field. *Soil Tillage Research, 103*, 302–309.

Diserens, E., Chanet M., Marionneau, A. (2010). Machine weight and soil compaction: TASC V2.0.xls – a practical tool for Decision-making in Farming. AgEng2010 – Clermont-Ferrand, 6-8 of September, Proceedings, Ref: 239, 1–10.

Diserens, E., & Steinmann, G. (2002). Calculation of pressure distribution in moist arable soil in eastern Switzerland: a simple model approach for the practice. In L. Vulliet, L. Laloui, & B. Schrefler (Eds.), *Environmental geomechanics* (pp. 413–421). EPFL Press.

Döll, H. (1999). Lohnen Zwillingsräder an Mähdreschern? Landwirtschaft ohne Pflug. *Sonderaufgabe Agritechnica*, 6–8.

Döll, H., & Schneider, T. (2001). Deformation characteristics of farm tires – effect on the soil pressure and the plant stress. *Conference Agricultural Engineering*, 8, VDI-MEG.

Eichhorn, H. (1999). *Landtechnik 7*. Auflage Ulmer Verlag.

Godin, T. (2005). Evaluation des contraintes engendrées par les engins dans les systèmes de grande culture, viticoles et forestiers français. Mémoire de fin d'étude. Ecole d'Ingénieurs de l'Esitpa.

Godin, T., Defossez P., Leveque, E., Le Bas, C., Boizard, H., Debuisson, S., et-al (2006). Evaluation des contraintes endgendrées par les engins dans les systèmes de grandes cultures, viticoles et forestiers français. Proceedings of the 69th congress – Brussels, 15–16 February.

Gourves, R. (1996). Pénétromètre dynamique léger à énergie variable: PANDA. *Sol SOLUTION*, . notice technique no. 04–2410b, (Romagnat, France).

Grecenko, A. (1995). Tyre footprint area on hard ground computed from catalogue value. *Journal of Terramechanics, 32*(6), 325–333.

Gregory, A. S., Watts, C. W., Whalley, W. R., Kuan, H. L., Griffiths, B. S., Hallett, P. D., et al. (2007). Physical resilience of soil to field compaction and the interactions with plant growth and microbial community structure. *European Journal of Soil Science, 58*, 1221–1232.

Hallonborg, U. (1996). Super ellipse as tyre-ground A. *Journal of Terramechanics, 33*(3), 125–132.

Heinonen, M., Alakukku, L., & Erkki, A. (2002). Effects of reduced tillage and light tractor traffic on the growth and yield of oats. In M. Pagliai, & R. Jones (Eds.), *Sustainable land management-environmental protection. Advances in geoecology, Vol. 35* (pp. 367–378). Reiskirchen: Catena Verlag.

Horn, R., Domzal, H., Slowinska-Jurkiewicz, A., & van Ouverkerk, C. (1995). Soil compaction processes and their effects on the structure of arable soils and the environment. *Soil Tillage Research, 35*(2–3), 277–304.

Inns, F. M., & Kilgour, J. (1978). *Agricultural tyres*. London: Dunlop. 69 pp.

Jones, R. J. A. (2002). Assessing the vulnerability of soils to degradation. In M. Pagliai, & R. Jones (Eds.), *Sustainable land management-environmental protection. Advances in geoecology, Vol. 35* (pp. 33–44). Reiskirchen: Catena Verlag.

Keller, T. (2005). A model for the prediction of the A and the distribution of vertical stress below agricultural tyres from readily available tyre parameters. *Biosystems Engineering, 92*(1), 85–96.

Komandi, G. (1990). Establishment of soil-mechanical parameters which determine traction on deforming soil. *Journal of Terramechanics, 72*(2), 115–124.

Lines, J. A., & Murphy, K. (1991). The stiffness of agricultural tractor tyres. *Journal of Terramechanics, 28*(1), 49–64.

McKyes, E. (1985). *Soil cutting and tillage, Vol. 7*. Amsterdam, Netherlands: Elsevier. Developments in Agricultural Science.

O'Sullivan, M. F., Henshall, J. K., & Dickson, J. W. (1999). A simplified method for estimating soil compaction. *Soil Tillage Research, 49*, 325–335.

O'Sullivan, M. F., Robertson, E. A. G., & Henshall, J. K. (1999). Shear effects on gas transport in soil. *Soil Tillage Research, 50*, 73–83.

Rempfer, M. (1998). Grundlagen der automatischen Reifenluftdruckverstellung bei landwirtschaftlichen Fahrzeugen. *Agrartechnische Forschung, 4*(1), 46–55.

Söhne, W. (1953). Druckverteilung im Boden und Bodenverformung unter Schlepperreifen. Grdlgn. d. *Landtechn. Heft, 5*, 49–62.

Schjønning, P., Lamandé, M., Tøgersen, F. A., Arvidsson, J., & Keller, T. (2008). Modelling effects of tyre inflation pressure on the stress distribution near the soil-tyre interface. *Biosystems Engineering, 99*, 119–133.

Schwieger, H. (1996). Untersuchung neuartiger Laufwerke und lasergestützte Erfassung der Reifen- / Bodenverformung. Forschungsbericht Agrartechnik des Arbeitskreises Forschung und Lehre der Max-Eyth-Gesellschaft Agrartechnik (VDI-MEG) Dissertation Kiel. 165 pp.

Smith, D. L. O. (1985). Compaction by wheels: a numerical model for agricultural soils. *Journal of Soil Science, 36*, 621–632.

Soane, B. D., & van Ouwerkerk, C. (1994). Soil compaction problems in world agriculture. In B. D. Soane, & C. van Ouwerkerk (Eds.), *Soil compaction in crop production* (pp. 1–21). Elsevier, 662 pp.

Steiner. M, (1979). Analyse, Synthese und Berechnungsmethoden der Triebkraft-Schlupf-Kurve von Luftreifen auf nachgiebigem Boden. Forschungsbericht Agrartechnik des Arbeitskreises Forschung und Lehre der Max-Eyth-Gesellschaft (MEG) 33. Dissertation Munich. 190 p.

Tobias, S., Schulin, R., Schaub, D., Weisskopf, P., Buchter, B., Zimmermann, S., et al. (1999). *Physikalischer Bodenschutz, Vol. 9*. Bodenkundliche Gesellschaft der Schweiz BGS Dokument.

Van den Akker, J. J. H. (1998). Development, verification and use of the subsoil compaction model Socomo. Proceedings of the 1st workshop of the Concerted Action on subsoil compaction, 28–30 may 1998, Wageningen, The Netherlands. 17 p.

Walczak, R., Orlowski, R., & Pukos, A. (1973). A manual spring penetrometer of soil with recorder. *Polish Journal of Soil Science, 2*, 87–94.